BMES
BIOMEDICAL ENGINEERING SOCIETY™
www.bmes.org

CrossMark

Medical Stents: State of the Art and Future Directions

A Review of Material Degradation Modelling for the Analysis and Design of Bioabsorbable Stents

Enda L. Boland, Connor J. Shine, Nicola Kelly, Caoimhe A. Sweeney, and Peter E. McHugh

Biomechanics Research Centre, Biomedical Engineering, National University of Ireland Galway, University Road, Galway, Ireland

Associate Editor Sean McGinty oversaw the review of this article.

Abstract—The field of percutaneous coronary intervention has witnessed many progressions over the last few decades, more recently with the advancement of fully degradable bioabsorbable stents. Bioabsorbable materials, such as metallic alloys and aliphatic polyesters, have the potential to yield stents which provide temporary support to the blood vessel and allow native healing of the tissue to occur. Many chemical and physical reactions are reported to play a part in the degradation of such bioabsorbable materials, including, but not limited to, corrosion mechanisms for metals and the hydrolysis and crystallization of the backbone chains in polymers. In the design and analysis of bioabsorbable stents it is important to consider the effect of each aspect of the degradation on the material's *in vivo* performance. The development of robust computational modelling techniques which fully capture the degradation behaviour of these bioabsorbable materials is a key factor in the design of bioabsorable stents. A critical review of the current computational modelling techniques used in the design and analysis of these next generation devices is presented here, with the main accomplishments and limitations of each technique highlighted.

Keywords—Finite element analysis, Computational modelling, Biodegradable stent, Corrosion, Polymer, Hydrolysis, Magnesium.

INTRODUCTION

Coronary stents have revolutionised the treatment of coronary artery disease. While coronary artery stenting is now relatively mature, significant scientific and technological challenges still remain, particularly in tackling the complications associated with long-term placement of the device. One of the most fertile technological growth areas is bioabsorbable stents. It is now possible to generate stents that will break down in the body once the initial necessary scaffolding period (6–12 months)[29] is complete and which can promote arterial remodelling.[11] Bioabsorable stents have so far been designed from either metal or polymer materials (Table 1). Such technologies permit the use of repeat treatments (surgical or percutaneous) to the same site[41] and have potential for use in areas of complex anatomy, where a conventional stent would permanently obstruct side branches,[41] or for paediatric patients[74] where a conventional stent may become mechanically unstable in growing vessels. Bioabsorable stents present possibilities for the controlled local delivery of antiproliferative drugs, which could reduce the need for long-term use of antiplatelet therapy. Ultimately, bioabsorbable stents possess great potential in addressing the long-term clinical problems associated with permanent stents, such as in-stent restenosis,[35] late stent thrombosis[40] and stent fatigue fracture[61] while effectively allowing the restoration of vasomotion potential.

From the perspective of designing next generation bioabsorable stents, the phenomenon of biodegradation, through either surface corrosion in the case of metals[25] or bulk degradation in the case of polymers,[54] adds significant complications, in comparison to permanent stents. For example, capturing the effects of the *in vivo* environment, (dynamic loading, blood-flow, tissue remodelling *etc.*) on the rates of degradation or corrosion with computational techniques is a challenging task.

Address correspondence to Enda L. Boland, Biomechanics Research Centre, Biomedical Engineering, National University of Ireland Galway, University Road, Galway, Ireland. Electronic mail: e.boland1@nuigalway.ie
Enda L. Boland and Connor J. Shine contributed equally to the article.

TABLE 1. Summary of the bioabsorbable scaffolds that have undergone and are still in clinical evaluation.

Device name (Company)	Strut material	Strut thickness	Radio-opacity	Drug eluting	Crossing profile	Radial support	Resorption time	Current status
AMS-1 (Biotronik)	Magnesium alloy	165 μm	✗	✗	1.2 mm	Weeks	<4 months	Discontinued
DREAMS-1 (Biotronik)	Magnesium alloy	120 μm		✓—Paclitaxel	N/A*	3–6 months	9 months	Discontinued
DREAMS-2 (Biotronik)	Magnesium alloy	125 μm	Mettalic markers	✓—Sirolimus	N/A*	3–6 months	9 months	Clinical trial
Igaki-Tamai (Kyoto Medical)	Poly(L-lactide)	170 μm	Gold markers	✗	N/A	6 months	24 months	CE mark (Peripheral device)
ABSORB BVS 1.0 (Abbott Vascular)	Poly(L-lactide) and poly(D-lactide) coating	156 μm	Platinum markers	✓—Everolimus	1.4 mm	Weeks	18–24 months	Discontinued
ABSORB BVS 1.1 (Abbott Vascular)	Poly(L-lactide) and poly(D-lactide) coating	156 μm	Platinum markers	✓—Everolimus	1.4 mm	6 months	18–24 months	CE mark
ABSORB GT1 (Abbott Vascular)	Poly(L-lactide)	156 μm	Platinum markers	✓—Everolimus	1.4 mm	6 months	18–24 months	CE mark
REVA (Reva Medical)	Poly-tyrosine derived polycarbonate	200 μm	Scaffold	✗	1.7 mm	3–6 months	24 months	Discontinued
ReZolve (Reva Medical)	Poly-tyrosine derived polycarbonate	200 μm	Scaffold	✓—Sirolimus	1.5 mm	4–6 months	24 months	In clinical trials
Fantom (Reva Medical)	Poly-tyrosine derived polycarbonate	114–228 μm	Scaffold	Not known	1.5 mm	4–6 months	24 months	In clinical trials
Pure Bioresorbable Scaffold (ART)	Poly(L-lactide)	170 μm	✗	✗	N/A*	3–6 months	3–6 months	CE mark
Fortitude (Amaranath Medical)	Poly(L-lactide)	150–200 μm	✗	✗	N/A*	3–6 months	3–6 months	In clinical trials
DESolve and DESolve 100 (Elixir)	Poly(L-lactide)	150 μm	Metallic markers	✓—Myolimus	1.5 mm	N/A	12–24 months	CE mark
Ideal BTI (Xenogenics)	Poly(L-lactide) and salicylates	200 μm	✗	✓—Sirolimus	1.5–1.7 mm	3 months	6–9 months	FIM completed. Discontinued
Ideal BioStent (Xenogenics)	Poly(L-lactide) and salicylates	150 μm	✗	✓—Sirolimus	1.5–1.7 mm	3 months	6–9 months	Pre-clinical stage
Acute BRS (Orbus Neich)	Poly(L-lactide), poly(D-lactide) and e-caprolactone	150 μm	Distal and proximal	✓—EPC and sirolimus	N/A	N/A	N/A	Pre-clinical stage
Xinsorb (Huaan Biotech)	Poly (L-lactide)	160 μm	Distal and proximal	✓—Sirolimus	N/A	N/A	N/A	Pre-clinical stage

AMS Absorbable magnesium scaffold, *BVS* bioresorbable vascular scaffold, *CE* Conformité Européenne, *GT1* GlideTrack catheter, *ART* arterial remodelling technologies, *FIM* first in man, *N/A** 6-Fr compatible, *EPC* endothelial progenitor cells.

This has implications for the development and use of computational modelling for bioabsorbable stents, as part of the analysis and design process.[22,73] This article aims to review the state of the art in computational modelling of material degradation in metallic and polymeric bioabsorable stents, to highlight accomplishments and limitations to date, and to indicate future advancements in this area.

A review of the literature shows that metals such as magnesium alloys[27,66,74] and iron alloys[45,67] and polymers such as Poly(L-lactic acid) PLLA,[19,62] Poly(lactic-co-glycolic acid) PLGA[38] and Polycaprolactone, PCL[63] have been the materials most commonly investigated for use in bioabsorable stents. For convenience, the terms resorbable metal stents (RMS) and resorbable polymer scaffolds (RPS) are used in this review to prevent confusion with commonly used trade names AMS and BVS, in reference to the Biotronik absorbable metallic stent and Abbott bioresorbable vascular scaffold, respectively.

Metals generally have superior mechanical stiffness and strength compared to polymers, an attractive characteristic for use in load bearing applications such as coronary stents. Magnesium and iron based alloys are considered favourable materials for RMS as they both are naturally present in the human body, have good biocompatibility and have degradation products which do not cause toxicity.[29,75]

Problems associated with iron-based RMS include incompatibility with certain imaging devices (MRI) and slow *in vivo* degradation rates as reported in preliminary animal studies.[44,75] To the best of the authors knowledge iron-based RMS have not proceeded beyond animal trail stage, whereas magnesium-based RMS have progressed significantly faster with Biotronik presently conducting their third clinical trial of these devices (Table 1).[5,27,66] Due to this relative advancement and clinical trial promise, and given that iron stents would behave mechanically like permanent stents in the short to medium term, computational modelling (using finite elements (FE)) of RMS degradation has focused on magnesium alloy stents.

Some of the problems associated with RMS, for example high thrombogenicity due to electropositive charges and fast degradation rates of magnesium RMS, can be bypassed with the development of RPS, that typically would degrade more slowly (18–24 months).[1] While RPS typically have thicker struts than RMS, no direct evidence linking strut thickness to restenosis rates has yet been found for the current bioabsorbable technologies.[14] The microstructural properties of polymer materials make them ideal carriers for drugs for the purpose of controlled release, which was in itself a contributing factor in the development of polymer coatings on permanent stents.[38]

Biodegradable polymers are of increasing interest in biomaterials research and PLLA has been extensively investigated for medical applications since 1970[63] due to its excellent biocompatibility and physiochemical properties, which are easily tuned through the manufacturing process.[63] This material has successfully been employed in Abbott's Absorb BVS,[19,42] the DESolve scaffold[64] and the device from Arterial Remodelling Technologies[11] which have all obtained market approval in Europe. A number of other RPS devices are currently undergoing pre-clinical or clinical investigation, as shown in Table 1. For the stent application, therefore, computational modelling has primarily focused on PLLA degradation and mechanical behaviour.[6]

DEGRADATION OF MATERIALS

Degradation of Metals

A detailed description of magnesium degradation through corrosion can be found in Song and Atrens.[60] Magnesium alloys when implanted *in vivo* corrode by various mechanisms including but not limited to: (a) micro-galvanic corrosion, (b) localised (pitting) corrosion, (c) intergranular corrosion, (d) stress corrosion cracking and (e) corrosion fatigue. For the stent application, modelling to date has been predominantly focused on representing micro-galvanic corrosion and localised (pitting) corrosion in magnesium alloys, both of which are described briefly below.

Magnesium alloys are highly susceptible to micro-galvanic corrosion. Mirco-galvanic corrosion is an electrochemical process where magnesium (anode), alloying elements or impurities (cathode) and an electrolyte form a galvanic cell, resulting in heavy localised corrosion adjacent to the cathode. Metals with low hydrogen overvoltage, including Ni, Fe, and Cu cause severe galvanic corrosion of magnesium alloys while others such as Al, Zn, Cd, and Sn, are much less damaging.[60]

Magnesium is a naturally passive metal that undergoes pitting corrosion at its free corrosion potential, when exposed to chloride ions in a non-oxidizing medium. As a result, the corrosion of magnesium alloys in neutral or alkaline salt solutions typically takes the form of pitting.[60]

Degradation of Polymers

Polymer degradation can occur through a number of mechanisms including mechanical, thermal, photon and chemical (biological and/or enzymatic) driven means. Synthetic polymers such as PLLA belong to the

family of biodegradable aliphatic polyesters. Such biodegradable polymer materials undergo degradation *in vivo* through a two-phase process, beginning with chemical hydrolysis, where the vulnerable bonds in the polymeric chain react with water molecules and are broken down into oligomers and then into monomer fragments.[20] This hydrolysis is often considered an autocatalytic process, as chain scission of the backbone chains leads to the formation of carboxyl end groups, which increase the acidic environment and therefore accelerate the rate of hydrolytic breakdown.[47] Degradation through hydrolysis is considered a passive process; it does not require the presence of enzymes and it is governed principally by water molecules penetrating the device.[69]

The second phase of *in vivo* degradation involves active metabolism reactions, where the newly formed monomer fragments are converted into non-toxic products, i.e., lactic acids, which are then easily excreted from the body through normal cellular activities.[68] Hydrolysis mechanisms in biodegradable polymers have been studied extensively and it is imperative that both the chemical and physical aspects are considered when describing or modelling this complicated process.[33]

COMPUTATIONAL MODELS FOR MATERIAL DEGRADATION

Metallic Degradation Models

A brief overview and key equations of degradation models applied to RMS is provided in Table 2. A detailed description is provided in the following sections.

Uniform Corrosion Modelling

Uniform corrosion modelling, where corrosion is considered to occur at a uniform rate over the exposed surface of the RMS, is perhaps the simplest form of RMS degradation modelling, and is an approximate representation of micro-galvanic corrosion for magnesium alloys if the distribution of alloying elements in the material is considered to be homogeneous.[18] Gastaldi *et al.*[18] and Grogan *et al.*[25] used a continuum damage mechanics (CDM) approach to simulate uniform corrosion in RMS FE models by employing sequential finite element removal from the exterior surface of the RMS. Grogan *et al.*[22] developed this further to model uniform corrosion using on arbitrary Lagrangian–Eulerian (ALE) adaptive meshing technique.

The CDM methodology introduces a local dimensionless damage parameter D which accounts for the loss of mechanical integrity of the stent material due to corrosion. In the FE context, for a partially corroded

TABLE 2. Summary of material degradation models that have been used to investigate the performance of bioabsorbable metallic stents.

Authors	Model type	Brief description	Key equations	Code
Gastaldi et al.[18]	Phenomenological-uniform corrosion	Element deletion model using CDM methodology by introducing damage parameter for uniform corrosion D_U and effective Cauchy stress tensor $\tilde{\sigma}_{ij}$	$\sigma_{ij} = \tilde{\sigma}_{ij}(1-D)$ $\frac{dD_U}{dt} = \frac{\delta_U}{L_e}k_U$	Abaqus/Explicit (VUSDFLD)
Gastaldi et al.[18]	Phenomenological-stress corrosion	Element deletion model using CDM methodology by introducing damage parameter for stress corrosion D_{SC} and effective Cauchy stress tensor $\tilde{\sigma}_{ij}$. Stress corrosion activated if equivalent stress is greater than threshold stress	$\sigma_{ij} = \tilde{\sigma}_{ij}(1-D)$ $\frac{dD_{SC}}{dt} = \frac{L_e}{\delta_{SC}}\left(\frac{S\sigma^*_{eq}}{1-D_{SC}}\right)^R$ When $\sigma^*_{eq} \geq \sigma_{th} \geq 0$	Abaqus/Explicit (VUSDFLD)
Grogan et al.[25]	Phenomenological-uniform corrosion	Element deletion model using CDM methodology by introducing damage parameter for uniform corrosion D_U and effective Cauchy stress tensor $\tilde{\sigma}_{ij}$	$\sigma_{ij} = \tilde{\sigma}_{ij}(1-D)$ $\frac{dD_U}{dt} = \frac{\delta_U}{L_e}k_U$	Abaqus/Explicit (VUMAT)
Grogan et al.[25]	Phenomenological-pitting corrosion	Element deletion model using CDM methodology by introducing damage parameter for uniform corrosion D_P and effective Cauchy stress tensor $\tilde{\sigma}_{ij}$	$\sigma_{ij} = \tilde{\sigma}_{ij}(1-D)$ $\frac{dD_P}{dt} = \frac{\delta_U}{L_e}\lambda_e k_U$	Abaqus/Explicit (VUMAT)
Grogan et al.[23,24]	Phenomenological-uniform corrosion	ALE model utilising adaptive meshing which allows boundaries of the FE mesh to be moved independently. Corrosion rate directly inputted as velocity of moving stent surface.	–	Abaqus/Standard (UFIELD, UEXTERNALDB, UMESHMOTION)
Grogan et al.[23,24]	Physical-uniform corrosion	Physical model based on the diffusion of metallic ions from the surface of the stent. Velocity of the moving stent surface depends on metallic ion concentration gradient.	$v = \frac{D_{ion}(\nabla c \cdot n)}{c_{sol} - c_{sat}}$	Abaqus/Standard (UFIELD, UEXTERNALDB, UMESH-MOTION)

finite element, the elemental Cauchy stress σ_{ij} (the stress at the integration point, assuming a single integration point per 3D element) is related to the effective Cauchy stress (the stress in the remaining uncorroded material within the element) $\tilde{\sigma}_{ij}$ through the following:

$$\sigma_{ij} = \tilde{\sigma}_{ij}(1 - D) \tag{1}$$

Initially when $D = 0$ the material in the element is undamaged and as corrosion progresses, D increases. When $D \approx 1$ the material is completely corroded and is no longer able to support stress ($\sigma_{ij} = 0$) and the element is removed from the model. This model is applied to surface elements exposed to the corrosive environment, and in turn to the elements in the new surface that is generated by element removal. In the particular case of uniform corrosion, the evolution of the (uniform) damage parameter D_U for surface elements is given by:

$$\frac{dD_U}{dt} = \frac{\delta_U}{L_e} k_U \tag{2}$$

where k_U is the material corrosion kinetic parameter (dimensions $[T^{-1}]$), δ_U and L_e are the respective material and FE model characteristic lengths that are introduced to reduce mesh sensitivity. The approach was implemented in Abaqus/Explicit (DS SIMULIA, USA) by both groups through user subroutines VUSDFLD (Gastaldi et al.[18]) and VUMAT (Grogan et al.[25]). The models were initially calibrated using results from in vitro immersion tests of magnesium alloy samples. Gastaldi et al.[18] tested mass loss of cylindrical samples of five commercially available alloys. Grogan et al.[25] recorded the mass loss rate of thin rectangular films of magnesium alloy AZ31 in load free and uniform tension states. Both calibrated uniform corrosion models accurately replicated the mass loss rates observed experimentally.

An arbitrary Lagrangian–Eulerian (ALE) implementation of the uniform corrosion model was presented by Grogan et al.[22] as part of a geometrical optimisation strategy applied to RMS to highlight how scaffolding ability of these devices can be prolonged by enhancing stent design. This approach utilises adaptive meshing which allows the boundaries of the FE mesh to be moved independently of the underlying material between analysis increments. This simulates the effects of material removal, as any material outside of the FE mesh in an increment does not contribute to mechanical behaviour, and the nodes on the external surface move at a velocity equal to the corrosion rate (in the form $[LT^{-1}]$) of the material. Grogan et al.[22] used Abaqus/Standard (DS SIMULIA, USA) with UFIELD, UEXTERNALDB and UMESHMOTION user subroutines. This approach is attractive as it is more efficient and less mesh sensitive than the element removal approaches, however less flexible in accounting for complex geometrical changes that may occur in localised corrosion representations.[25]

Uniform corrosion has been demonstrated to represent the best case scenario for RMS degradation, in terms of arterial scaffolding duration, in comparison to more inhomogeneous and localised corrosion mechanisms.[22,25] The above formulations, while simple to implement and powerful in simulating how an RMS would optimally perform, as presented,[18,22,25] do not account for the reality of localised surface corrosion or the possibility of stress modulated corrosion because they are controlled by a prescribed uniform material corrosion rate. Enhanced formulations that address such issues are summarised below.

Stress Corrosion Modelling

Gastaldi et al.[18] presented a Stress Corrosion (SC) model (implemented in Abaqus/Explicit) adapted from the work of da Costa-Mattos et al.,[10] who used CDM to create a model to describe the damage induced by SC in austenitic stainless steel. The evolution equation for the damage parameter in this (stress corrosion) case D_{SC} is:

$$\frac{dD_{SC}}{dt} = \frac{L_e}{\delta_{SC}} \left(\frac{S\sigma_{eq}^*}{1 - D_{SC}} \right)^R \tag{3}$$

when $\sigma_{eq}^* \geq \sigma_{th} \geq 0$ and $\frac{dD_{SC}}{dt} = 0$ when $\sigma_{eq}^* < \sigma_{th}$, where δ_{SC} and L_e are the respective material and FE model characteristic lengths, R and S are constants related to kinetics of the SC process and σ_{eq}^* is the equivalent stress for the SC mechanism (maximum principal stress in this case). If the value of equivalent stress σ_{eq}^* is below a threshold stress σ_{th} the SC process does not occur. A threshold stress of 50% of the yield stress of magnesium alloy ZM21 was selected.[18]

Gastaldi et al.[18] coupled the SC model with the uniform corrosion model described previously and applied both corrosion mechanisms to RMS geometry. The initial results of the simulations were considered phenomenologically consistent with experimental observations. This coupled formulation was further studied by Wu et al.[71,72] who completed in vitro corrosion tests on two RMS designs (a patented stent design (CON) and an optimized stent design (OPT)) and compared results against simulated predictions for one ring models of the same designs, as shown in Fig. 1, validating the overall applicability and practical usefulness of the model in stent design and performance assessment.

However, magnesium alloys are subject to localised pitting corrosion in vivo.[3,70] Thus, the omission of the
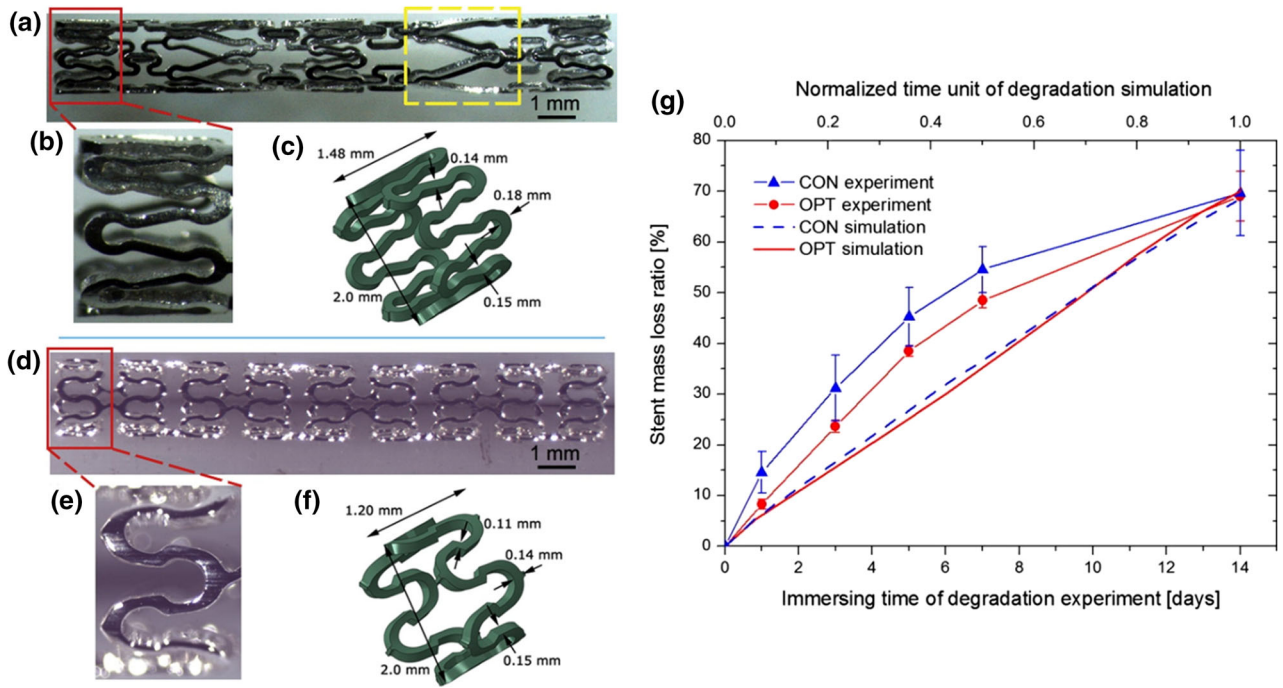
FIGURE 1. The original configuration of a CON sample (a, b) and an OPT sample (d, e). The dimensions of the CON and OPT models in the simulation (c, f) are shown. Note that the CON model only considered the short ring of the CON design. (g) Mass loss ratio of the CON and OPT samples for the experiment and the corresponding models for the simulations.[71]

pitting corrosion mechanism in the coupled uniform and SC approach may be considered a limitation.

Pitting Corrosion Modelling

Grogan *et al.*[25] presented a model for pitting corrosion by expanding on the aforementioned CDM uniform corrosion element removal model (implemented in Abaqus/Explicit) through the inclusion of a pitting parameter λ_e to capture the effects of localised or pitting corrosion. The evolution equation for the damage parameter in this (pitting corrosion) case D_P is:

$$\frac{dD_P}{dt} = \frac{\delta_U}{L_e} \lambda_e k_U \qquad (4)$$

Each element on the corrosion surface is randomly assigned a pitting parameter λ_e through the use of Weibull distribution-based random number generator.[25] An element assigned a larger value of λ_e degrades faster than its neighbours and nucleates a surface pit when removed ($D_P \approx 1$). Subsequently, the elements adjacent to the pit are assigned pitting parameters λ_e given by:

$$\lambda_e = \beta \lambda_n \qquad (5)$$

where λ_n is the pitting parameter of the pit nucleating element and β is a dimensionless parameter that controls the acceleration/deceleration of pit growth. In

Grogan *et al.*[25] the model parameters K_U, β and the Weibull probability distribution function were calibrated and the model quantitatively validated by comparison with results from three separate *in vitro* immersion experiments which measured the corrosion rate of magnesium alloy AZ31 foils in (i) load free, (ii) corrosion followed by tensile loading, and (iii) corrosion during tensile loading cases.[25] The pitting corrosion model was then applied to a stent geometry based on the Biotronik Magic stent and generated a stent degradation and collapse pattern that is qualitatively very similar to clinical trial observations for RMS, for example Waksman,[65] as highlighted in Fig. 2.

A limitation of the pitting corrosion formulation as presented[25] is the randomness of the location of pit nucleation. While pitting is certainly realistic,[60] pit locations are more than likely influenced by sites of surface defects from the manufacturing process, surface defects from angioplasty procedure, or areas of stress concentration as motivated by the aforementioned work of Wu *et al.*[71] who experimentally reported an increase in magnesium stent fractures in hinge regions.

Physically-Based Corrosion Modelling

The formulations presented above can be fundamentally classified as phenomenological, in that they
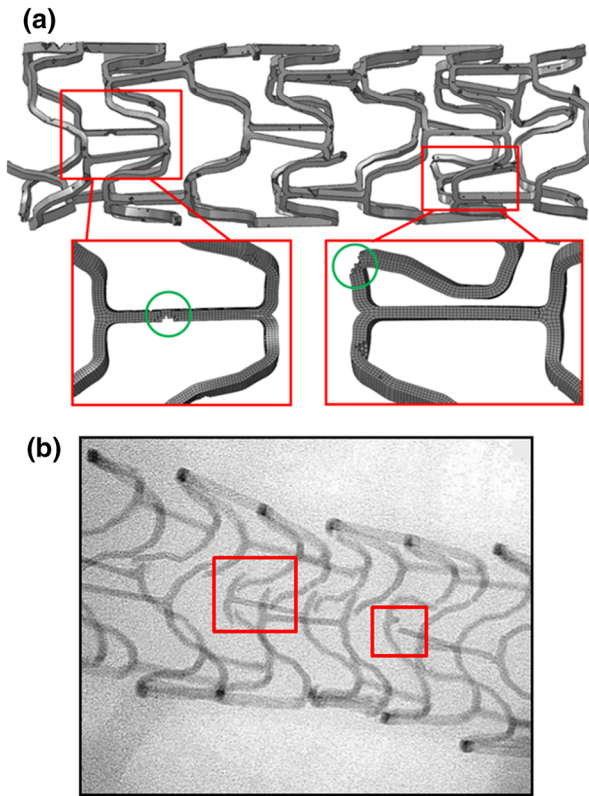
FIGURE 2. (a) Computational simulation of the magnesium stent subject to pitting corrosion model.[25] (b) *In vivo* image of Biotronik AMS stent 4 weeks after implantation.[65] Highlighted regions show qualitatively similar break regions due to corrosion.

capture the overall phenomena of degradation (and are quantitatively calibrated to generate realistically meaningful predictions) but do not explicitly represent the multi-physics processes generating the degradation. In an attempt to address this in the context of RMS analysis, Grogan *et al.*[23] presented a physically-based model that uses corrosion product (assumed to be magnesium ion) diffusion from the stent surface into a corrosive medium as the controlling variable for the corrosion process, coupled with corroding stent surface retreat. The model used an ALE approach similar to that described above for uniform corrosion, without the limitation that corrosion had to be strictly spatially uniform, and was implemented in Abaqus/Standard with UFIELD, UEXTERNALDB and UMESHMOTION user subroutines. The model was used to simulate the behaviour of a hypothetical pure magnesium RMS, on the basis that pure magnesium, although inferior in terms of mechanical properties,[16] has a greater tendency to corrode through diffusion controlled ion transfer rather than micro-galvanic corrosion, making the model more physically appropriate.

Using the ALE approach, the corrosion surface moves at a velocity v, determined through:

$$v = \frac{D_{\mathrm{ion}}(\nabla c \cdot \boldsymbol{n})}{c_{\mathrm{sol}} - c_{\mathrm{sat}}} \qquad (6)$$

where c_{sol} is the concentration of magnesium in the stent, c_{sat} is the saturation concentration of magnesium in the corrosive environment, D_{ion} is the diffusivity of magnesium ions in the corrosive environment, $(\nabla c \cdot \boldsymbol{n})$ is normal component of the magnesium ion concentration gradient vector ∇c, with $\boldsymbol{n}$ as the local normal vector to the corrosion surface. Figure 3a shows a contour plot of predicted magnesium ion concentration in the corrosive environment over time. As the device corrodes its dimensions are reduced. The initially sharp edges of the device are rounded as corrosion progresses, as shown in Fig. 3b.[23] This model gives interesting insight into RMS degradation including the prediction of a simple power-law dependence of RMS mass (and hence scaffolding ability) on time, controlled by D_{ion} and c_{sat}.

The model is efficient and usable in its own right, but from a practical perspective it could be used to calibrate the corrosion parameters (even as functions of time) in the simpler uniform corrosion formulation[18,25] described above to simulate RMS performance in different corrosive environments, at least for diffusion-controlled corrosion, given the practical usefulness of the uniform corrosion model (especially with stress dependence).[71] Limitations of the model as presented[23] include a focus on diffusion-control and a simple material system (pure magnesium) where micro-galvanic corrosion is less dominant. Multi-physics simulations for more complex magnesium alloys and the geometrical complexity of pitting would present challenges.

Polymer Degradation Models

The modelling techniques which have been presented to date for describing the degradation of RPS can be categorised as either phenomenological or physically-based, as described below, and summarised in Table 3.

Phenomenological Modelling

Phenomenological modelling approaches have been applied to RPS, with the primary focus of simulating the mechanical performance of the RPS and predicting its scaffolding ability. These methods have involved a CDM approach similar to that discussed previously, where a degradation parameter d is introduced to account for the loss of the material's mechanical integrity.

Following on from the degradation theory proposed by Rajagopal and Wineman,[51] Rajagopal *et al.*[50]

(a)

t = 0.00 hrs

t = 0.01 hrs

t = 0.12 hrs

t = 0.23 hrs

(b)

t = 0.00 hrs   t = 0.01 hrs   t = 0.12 hrs   t = 0.23 hrs
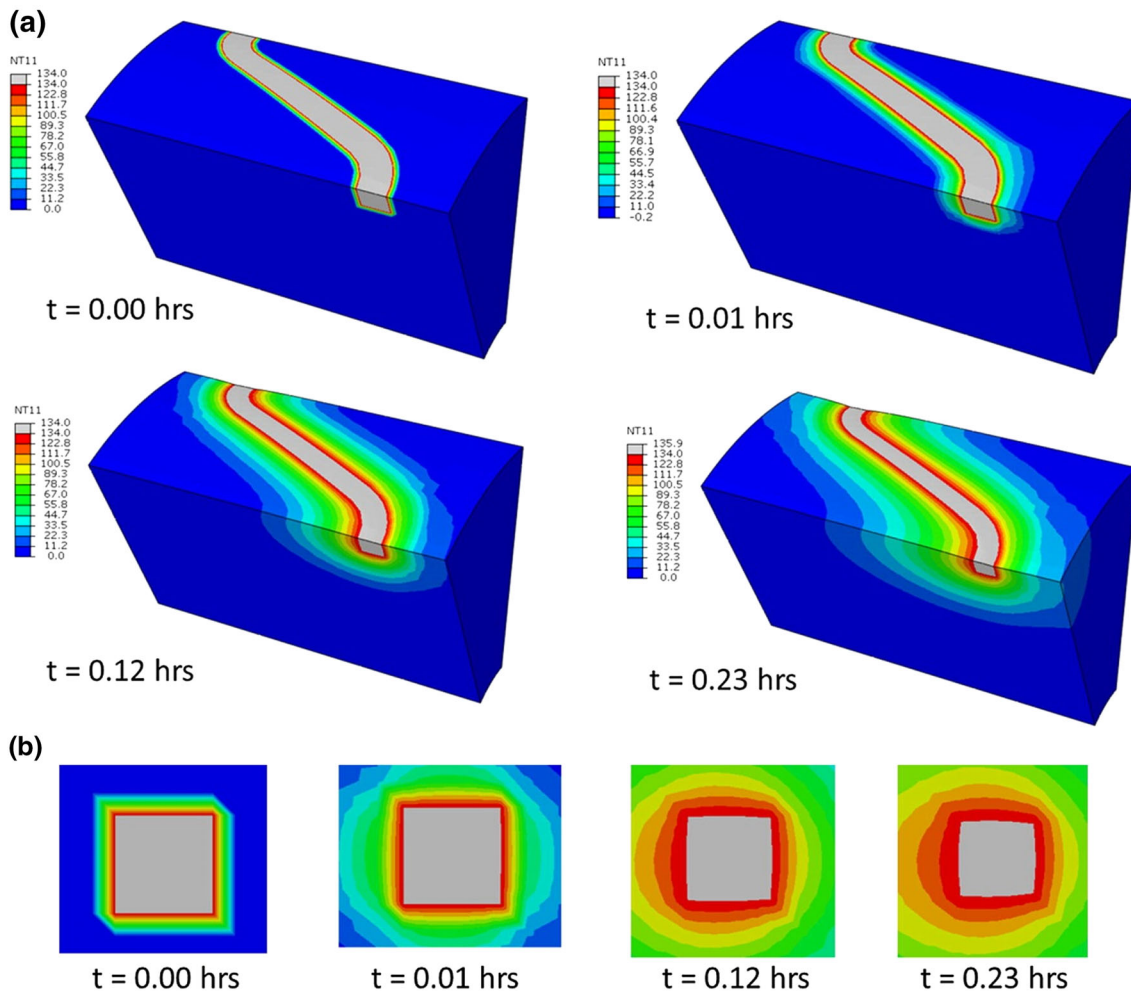
FIGURE 3.   Contour plots from the physical corrosion model of predicted magnesium ion concentration in kg m^{-3} in the corrosive environment over time. In (a) the upper half of the model has been removed for illustrative purposes. Grey regions correspond to non-corroded metal. (b) Illustration of the changing dimensions of a cross-section of the hinge as it corrodes.[23]

developed a thermodynamically consistent model for strain-induced degradation of rubbery polymers. Scission and healing (reformation of the networks) of the polymer chains were considered equally dependent on a state variable, which measured the extent of local degradation. This theory was further developed by Soares *et al.*[36,55–59] who reported a number of studies focusing predominantly on PLLA RPS. Variations in mechanical response due to degradation are captured through evolution of material parameters present in the chosen constitutive law. In their initial work,[55] a preliminary model was developed to describe the mechanical behaviour of a loaded, cylindrical structure composed of a linear degradable polymeric material. A degradation parameter d, essentially the same as the damage parameter described previously ($d = 0 \leftrightarrow$ no degradation; $d = 1 \leftrightarrow$ maximum degradation) was used. It was hypothesised in an earlier study,[50] that the rate of change of degradation was dependent on the

applied strain, the current state of degradation, and implicitly dependent on both spatial location and time, through the following relationship:

$$\frac{d}{dt}d(t) = C(1 - d(t))\left[(I_1 - 3)^2 + (I_2 - 3)^2\right]^{\frac{1}{2}} \quad (7)$$

where C is a time constant and I_1 and I_2 are the first and second strain invariants. In the constitutive model for the material, the strain energy was related to the degradation parameter through damage based evolution of the shear modulus μ as follows:

$$\mu = \mu_0(1 - d) \quad (8)$$

where μ_0 is the initial shear modulus.[55,58]

Results from experiments involving homogenous uniaxial extension of PLLA were then used to assess the predictions of the model. The model was first proposed for conditions of linear elastic behaviour and extended, in a follow up study,[57] to explain the non-

TABLE 3. Summary of material degradation models that have been used to investigate the performance of bioabsorbable polymeric stents.

Author	Model type	Brief description	Key equations	Code
Soares et al.[55,56]	Phenomenological-damage based	Degradation parameter related to the strain invariants of the deformation (I_1, I_2). Model incorporates degradation through degradation-dependent material properties	$\frac{d}{dt}d(t) = C(1-d(t))\left[(I_1-3)^2 + (I_2-3)^2\right]^{\frac{1}{2}}$ $\mu = \mu_0(1-d)$	Abaqus Standard (UMAT)
Muliana and Rajagopal[37]	Phenomenological-damage based	Modified viscoelastic QVL model to represent material behaviour. Degradation function defined in terms of the strain magnitude and concentration of water in the device and related to the material modulus E	$P(d,t) = \int_0^t E(d, \varphi^t - \varphi^s)\frac{dF}{d\varepsilon}\frac{d\varepsilon}{ds}\,ds$ $E(d,t) = E_\infty(1-\lambda_i d) + \sum_{n=1}^N E_n(1-\lambda_n d)e^{-\frac{t}{\tau_{Rt}}}$	Abaqus Standard (UMAT)
Khan and El-Sayed[30]	Phenomenological-damage based	Damage based model developed using combined Maxwell and Ogden-type models. Strain energy density ψ related to free energy of a single element, ψ^{el} of the ith Maxwell element ψ_i and the degradation parameter	$\psi(F, F_i^v, d) = \psi^{el}(F, d) + \sum_{i=1}^N \psi_i(FF_i^{v-1}, d)$	Abaqus Standard (UMAT)
Luo et al.[32]	Phenomenological-damage based	Model incorporates a degradation degree which was described using an exponential function. Material constants (a,b,c,m,n) obtained by fitting model to experimental data	$D = D(\varepsilon, t) = a(b + c\times\varepsilon^n)\times t^m$	Abaqus Standard (USDFLD)
Shazly et al.[53], Ferdous et al.[13]	Physical-transient diffusion reaction	First order degradation model developed based on transient diffusion–reaction equations for each polymer species $S_{(1-5)}$. Each species was described as a function of the hydrolysis K, auto-catalysis effects K_a and its stoichiometric coefficient n_{1-5}. Examined the local LA concentrations C_0^s using diffusion based model.	$S_1 \xrightarrow{K} n_2 S_2 \xrightarrow{K} n_3 S_3 \xrightarrow{K} n_4 S_4 \xrightarrow{K} n_5 S_5$ $\frac{\partial C_x^s}{\partial t} = f(K, K_a, C_{1-5}, n_{1-5})$ $\frac{\partial C_0^s}{\partial t} = \nabla\cdot(D_0^s \nabla C_0^s) + 2\sum_{m=1}^n kC_m^s A$	COMSOL (Multiphysics)
Prabhu et al.[48]	Physical-transient diffusion reaction	Simultaneous model of the biodegradation and drug release for a PLLA based stent coating. Presented four equations in terms of transport of the polymer (C_P which is shown on right), water molecules, oligomers and LA's	$\frac{\partial C_P}{\partial t} = \frac{\partial}{\partial x}\left(D_P \frac{\partial C_P}{\partial x}\right) - k_{PW}C_P C_W(1 + \alpha C_L)$	Not specified

QVL quasi linear viscoelastic, LA lactic acid, PLLA poly(L-lactic acid).

linear responses for finite deformations. As part of other work,[58] based on the results of experimental extension tests on un-degraded PLLA fibres, a specific form of the Helmholtz potential was used to represent the mechanical behaviour as follows:

$$\rho\psi(I_1, d) = \lambda(d)e^{-(I_1-3)}(I_1 - 3) + \mu(d)\ln[1 + a(I_1 - 3)]$$
(9)

where μ and λ are material properties that are both considered to be functions of the degradation d, ρ is the density and a is a material constant. This was implemented in Abaqus/Standard with user subroutines USDFLD and UHYPER to examine the behaviour of a RPS based on the Cypher stent geometry, (Fig. 4),[58] and investigated the effects of pressure on the degradation.

This model was extended by Muliana and Rajagopal[37] to describe materials which show viscoelastic characteristics in the absence of degradation. The degradation rate was modified to include the effects of water diffusion through the material and an adaptation of the quasi-linear viscoelastic (QLV) model[17] was used to form the constitutive law. Mate-
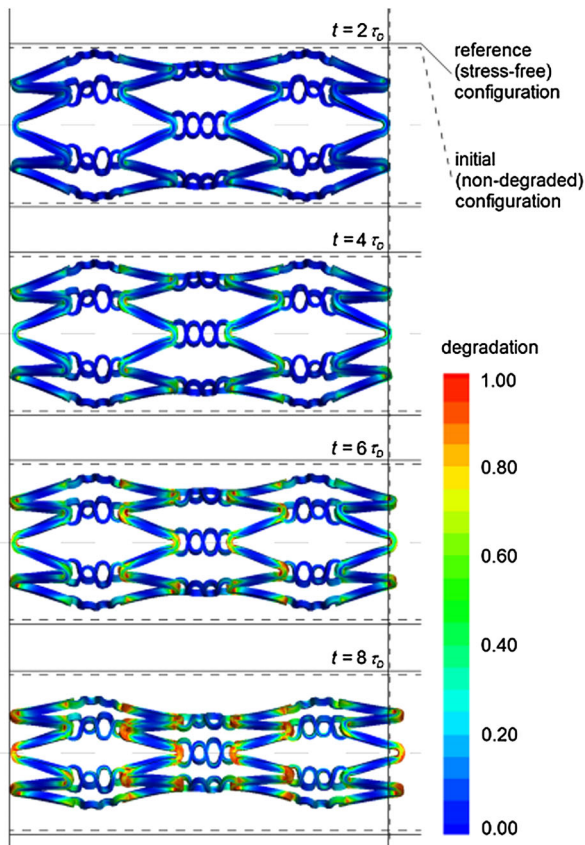

FIGURE 4. A biodegradable version of the Cypher stent was used to investigate the effects of pressurization on the magnitude and locations of degradation in a polymeric RPS, where time t is related to the characteristic time of degradation τ_D.[58]

rial parameters were calibrated and degradation of a PLLA RPS was examined using Abaqus/Standard and a UMAT user subroutine. The response of the polymer to quasi-static loading was examined and it was found that coupling between the scaffold and a viscoelastic arterial wall had a significant effect on the degradation response of the RPS. While this model presented an advanced methodology for studying the effects of degradation on the material's mechanical performance, the governing equation for water diffusion through the device was based on simple Fickian diffusion and a constant value was used for the water concentration, limiting the model's ability to accurately describe internal hydrolysis reactions. More recently, Hayman et al.[28] experimentally investigated how static and dynamic loading influenced the degradation of PLLA fibres and suggested exponential equations based on their results to describe the evolution of material properties for a Knowles's strain energy potential.

Khan and El-Sayed[30] utilized the previously described degradation parameter in the development of a non-linear visco-plastic model to predict the mechanical response of RPS under time-dependent loading conditions. The model was implemented in Abaqus/Standard and a study of two cylindrical annuli suggested that inhomogeneous deformations can occur in a RPS. A phenomenological model has also been presented by Luo et al.[32] who utilized combined experimental and numerical techniques to investigate the degradation behaviour of high molecular weight PLLA for use in RPS. Changes in the diameters of PLLA stents were measured following in vitro experimental testing and the ratios of elongation before and after degradation were used to define the degree of degradation. FE simulations using Abaqus/Standard (with USDFLD) were performed on a stent geometry; stress and strain distributions were seen to accumulate mainly at central locations of the stent and initial values reported for strain were related to the degradation rate of the material.

While the above models account for material degradation, and when implemented in FE software have demonstrated great capability for simulating the mechanical performance and scaffolding ability of a RPS, the formulations are phenomenological and rely for the most part on calibration of material parameters to macroscopic experimental material degradation data, and do not explicitly represent the internal physiochemical processes involved in the material degradation. This can be considered as a limitation, since elucidating the influence of these processes is a very important part of understanding RPS in vivo behaviour and is necessary for driving future RPS design. Physically-based models where such processes have been more explicitly represented are summarized below.

Physically-Based Modelling

Farrar and Buchanan[12] previously provided a summary of physically-based polymer degradation models and described how complex hydrolysis of the backbone bonds in biodegradable polyesters occurs at a molecular level within the material. Efforts have been made to model the most dominant physio-chemical processes involved in this phenomenon using continuum theory, and in particular, first-order kinetic equations have been proposed[47] to describe the diffusion of esters, monomers and water molecules. A recent example is the general degradation model of Wang et al.[68], where the evolution of ester bond and monomer concentrations are described by non-linear first-order rate equations, which incorporate autocatalytic rate constants, and where monomer diffusion is based on Fick's law.

Expanding on such an approach, Shazly et al.[53] presented a reaction-transport modelling framework to describe how the hydrolytic degradation of a tissue-embedded RPS affects the by-products released (implemented in COMSOL Multiphysics™). A 3D model was used to assess how the degradation rate, as well as arterial remodelling and metabolic activity rates, influenced the concentration of lactic acid (LA) present within arterial tissue. Degradation was modelled as a chain scission process and the concentrations of different polymer species C_{1-5}^S were related to the hydrolysis, K, and its autocatalytic effects, K_a, using equations of the form:

$$\frac{\partial C_i^s}{\partial t} = f(K, K_a, C_i, n_i), \quad i = 1, 2, 3, 4, 5 \qquad (10)$$

where n_i is the stoichiometric coefficient of each species. As part of further work, Ferdous et al.[13] explored the effects of scaffold structure and composition on the fate of the LA's and on the kinetics of the polymer degradation and erosion. Kinetic equations incorporating diffusion of the scaffold constituents were proposed, for example where C_j^s and D_j^s are the soluble constituent concentrations and the diffusion coefficient respectively, for a constituent with j ester bonds, and where k and A represent hydrolysis degradation and autocatalysis effects respectively, as follows:

$$\frac{\partial C_j^s}{\partial t} = \nabla \cdot \left(D_j^s \nabla C_j^s \right) - jkC_j^s A + 2 \sum_{m=j+1}^{n} kC_m^s A \quad 0 < j < 8$$
$$(11)$$

where n and C_m^s are, respectively, the number of ester bonds, and any constituent's concentration with the number of ester bonds between n and $j+1$ in the scaffold. A 2D computational model was developed using COMSOL (Fig. 5), with transport of soluble constituents through the arterial wall and the lumen governed by Eq. 11. Results from experimental

degradation studies on poly-dispersed PLLA were then used to validate the model. Scaffold degradation kinetics was found to have a major influence on the performance of PLLA-based RPS.

In terms of the material degradation models which have been developed for drug eluting polymer stents, Alexis[2] described the main factors that affect biodegradation and drug-release rate in the early 2000s. A number of research groups[8,43,48] have modelled the dual process of biodegradation and drug release for biodegradable stent coatings and RPS, using transport-reaction formulations, which accounted for the main physical–chemical parameters involved.

There is little evidence however, of physically-based models being developed with a focus on structural degradation of the RPS. Arosio et al.[4] used a "shrinking core" approach to develop a twinned drug release and degradation model, which was combined with a mechanical strength model for the analysis of resorbable polymer materials loaded with drugs. Decay of the polymer's mechanical properties, bending strength and tensile modulus, were related to the resistant section-area decrease and the molecular weight decrease respectively, however; this work was not specific to RPS. In general, the most advanced physically-based polymer degradation models that have been reported have predominantly been utilized for the analysis and design of general degradable polymeric devices and implants[26,31,34] other than RPS, as evidenced by the small number of studies of this type listed in Table 3. Therefore further work is needed to develop the equivalent modelling techniques for bioabosorbable stents. A model which encapsulates the dominant aspects of the hydrolytic degradation, while providing insight into the scaffold's mechanical integrity, would be of tremendous benefit to RPS development.

DISCUSSION AND RECOMMENDATIONS

According to FDA guidelines, FE analysis is required as part of the stent design process. However, specific guidelines relating to bioabsorbable stents have not yet been generated.[15] At present, while computational modelling techniques used to describe the degradation of metallic alloys and aliphatic polyesters consider the principal corrosion and hydrolysis mechanisms or the phenomenological effects of degradation on the materials mechanical behaviour, further work is needed to develop more comprehensive multi-physics and multi-scale modelling frameworks that combine the accuracy of the physically-based approach with the robust practicality of the phenomenological approach. Such advancements would have a significant impact on
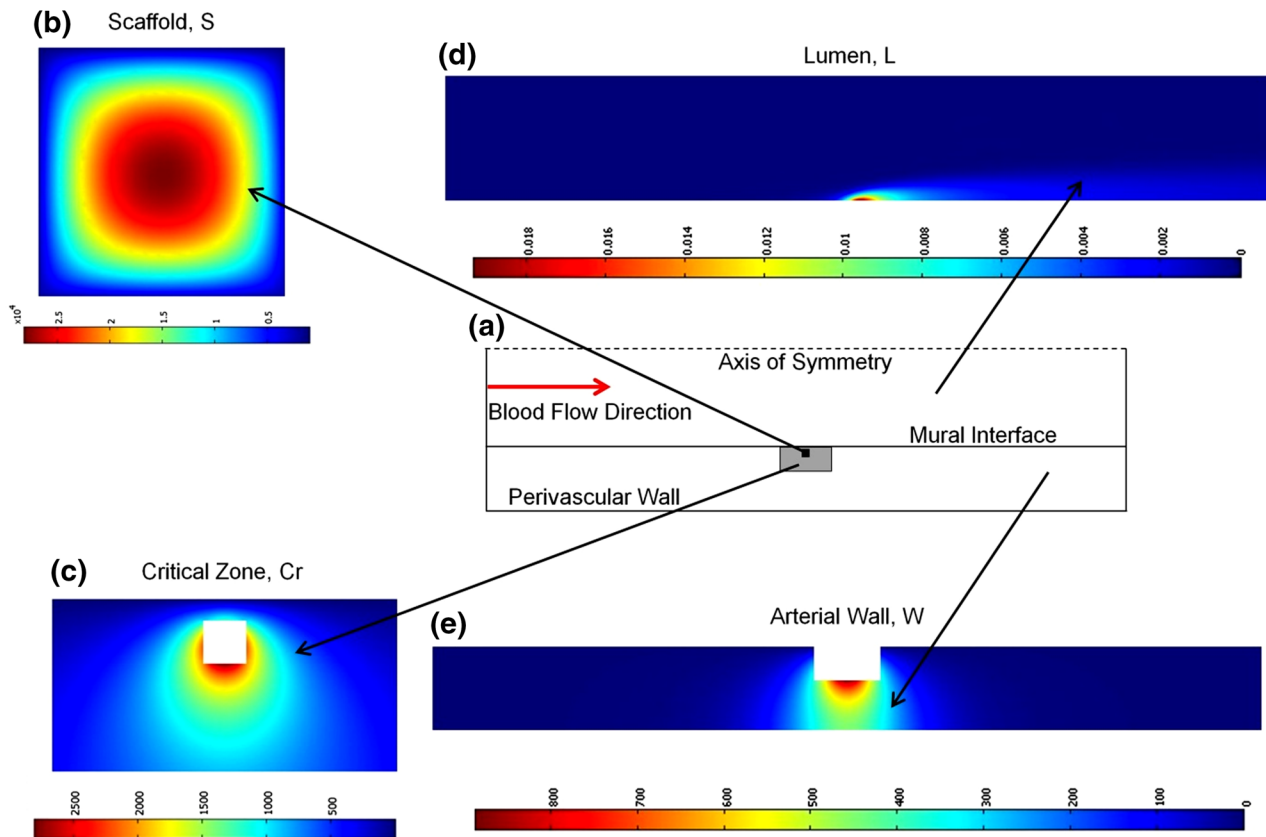
FIGURE 5. The schematic above shows the components of the two dimensional geometry used by Ferdous *et al.*[13] to represent a tissue-embedded PLLA scaffold. A diffusion reaction model was developed by the authors to investigate the degradation kinetics of the scaffold and the accumulation of lactic acids within the surrounding tissues.

the analysis and design of next generation bioabsorbable stents, and on the development of the regulatory guidelines surrounding these.

Undoubtedly, the development of bioabsorbable materials with superior performance in terms of mechanical properties and degradation behaviour is a critically important step in achieving more widespread use and enhanced clinical outcomes for bioabsorable stents.[7,75]

For the RMS, Chen *et al.*[7] suggested future work to develop the next generation magnesium-based materials that would include strategies such as alloying, processing, coating, development of novel porous magnesium scaffolds and development of metal-matrix composite materials. Computational modelling will form an integral part of this material development process, especially physically-based multi-scale modelling, where details of the dominant physio-chemical processes can be represented. For example, micromechanical models could be developed to build on the work of Grogan *et al.*[24] by combining a representation of microstructural deformation and corrosion at the granular level in magnesium.

For the RMS, as indicated previously, physically-based modelling should be extended to address microgalvanic corrosion and pitting corrosion for magnesium alloys. It could be used to calibrate the corrosion parameters (even as functions of time) in simpler phenomenological formulations[18,25] to simulate RMS performance in different corrosive environments, given the practicality of the phenomenological approach.

Due to its excellent biocompatibility and mechanical properties, PLLA has become widely used in medical devices and shows huge potential for the design of third generation vascular stents.[9] Attempting to capture each of the mechanical, morphological and thermal changes of a polymer as it undergoes chemical hydrolysis with a computational model is indeed challenging. Success in this depends on the availability of high quality experimental data to support the integration of degradation dependence on strain, temperature, processing and manufacturing techniques, crystallization and other physio-chemical processes into models specific to RPS. In terms of the phenomenological models, gaps still exist; where for example the simple inverse proportionality that is as-
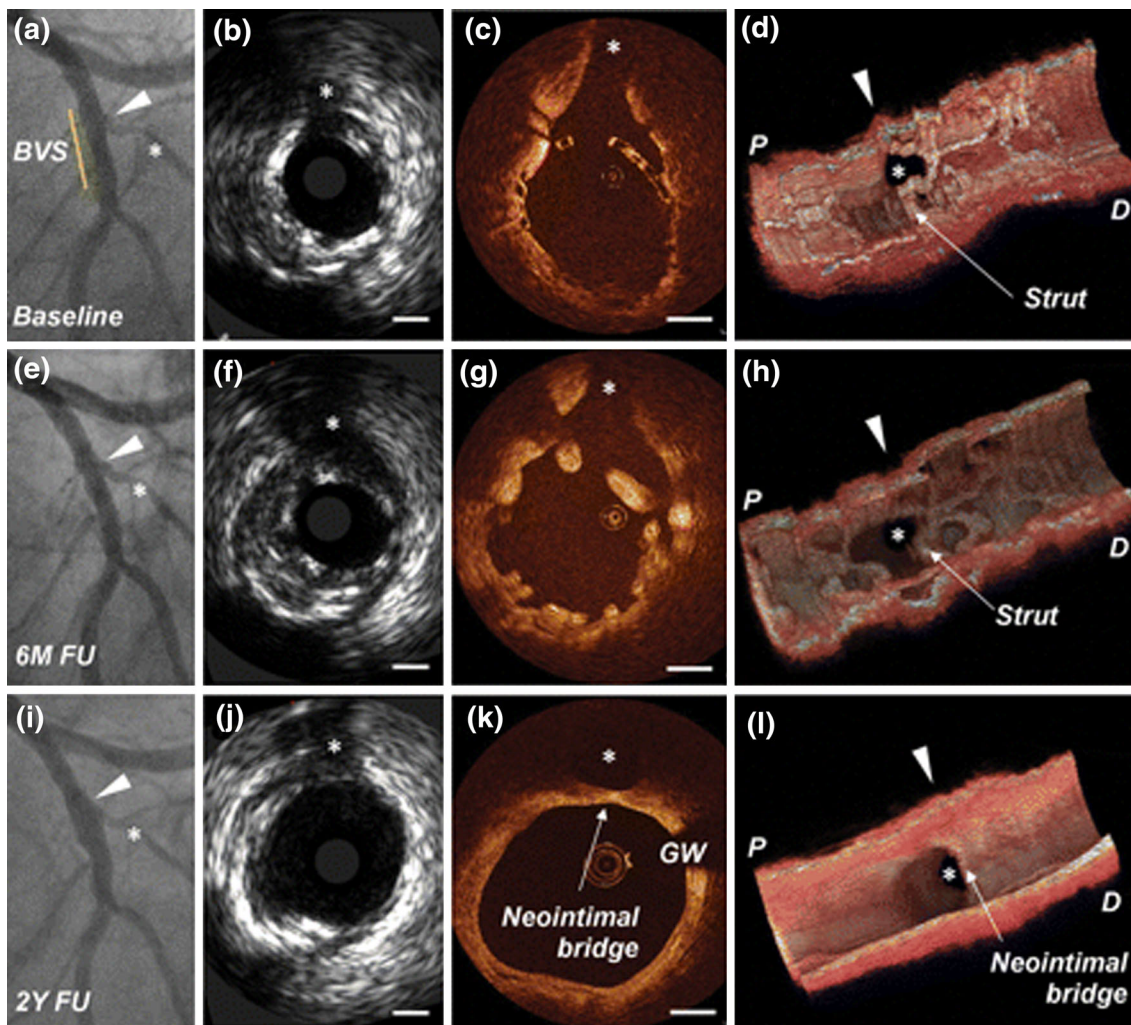
FIGURE 6. Diagnostic imaging techniques can be used to examine the degradation of bioabsorbable stents *in vivo*. Optical coherence tomography (OCT) and intravascular ultrasound (IVUS) results for the initial, 6 month and 2 year follow up of an implanted Abbott Vascular BVS 1.1 show good expansion of the BVS at baseline and the presence of neo-intimal tissue at 2 years. The structural changes which take place in the stent can also be easily observed using such imaging techniques. Image reprinted with permission from the author.[39]

sumed between induced damage and the changes in material properties[28] restricts the flexibility of the model. The inclusion of chemical processes involved in degradation would also allow such models to more realistically capture complex interactions between degradation and material behaviour. At present, the influence of different chain cleavage mechanisms, monomer diffusion and crystallization on the mechanical scaffolding ability of a RPS have not yet been evaluated.

Notably for the RPS, very few of the physically-based modelling techniques discussed previously consider an explicit representation of how the chemical reactions of degradation influence the mechanical response of the material. As previously stated for RPS, a physically-based model accounting for the dominant aspects of degradation, linked with a formulation that describes the

materials mechanical response, would be hugely beneficial in simulating the *in vivo* structural performance of a RPS to enhance future design and development.

The aim of computational modelling as a design tool for bioabsorable stents should be to replicate physiological conditions as accurately as possible. Combined with *in vivo* data, *in vitro* degradation experiments, which would more precisely mimic the clinical response of the device and where the *in vivo* environment is more accurately replicated, are required to calibrate and validate models. Suggested methods for improving on standard *in vitro* immersion tests used to quantify material degradation include the use of flow chambers[21] ideally with endothelial and/or smooth muscle cell attachment on the material surface.[52]

Cellular automata (CA) based modelling techniques are powerful methods to describe, simulate, and

understand the behaviour of complex physical systems.[46] CA has been previously used to simulate pitting corrosion of metals,[46] bulk erosion of polymers[8] and has been coupled with finite element methods to predict metallic grain structures and recrystallization.[49] Thus there is potential to use CA combined with finite element analysis to create physically based stent degradation models.

Advanced imaging techniques, such as intracoronary optical coherence tomography (OCT), should be more widely used to obtain *in vivo* data in relation to the condition of the bioabsorbable stent (scaffold area, stent fracture, corrosion product development) and coronary artery (lumen area, neo-intimal thickness) post deployment and at intermittent follow-up times (Fig. 6).[39]

Furthermore, OCT images such as Fig. 6 highlight the need to develop more realistic computational models which simulate *in vivo* phenomena such as remodelling of the arterial tissue around the stent struts and the formation of corrosion/degradation products from the stent. The inclusion of corrosion/degradation products is perhaps particularly important for RMS, where degradation is a surface based phenomenon involving the formation of substances such as magnesium hydroxide, in contrast to the RPS where bulk erosion through chemical hydrolysis is the primary form of degradation. The inclusion of degradation products in the computation models may well have an influence on the mechanical performance of the degrading stent. Also degradation products could have potential biological effects on the host metabolic system; however the representation of such effects in a computational model would be very challenging.

REFERENCES

[1]Agrawal, C. M., K. F. Haas, D. A. Leopold, and H. G. Clark. Evaluation of poly(L-lactic acid) as a material for intravascular polymeric stents. *Biomaterials* 13:176–182, 1992.

[2]Alexis, F. Factors affecting the degradation and drug-release mechanism of poly(lactic acid) and poly[(lactic acid)-co-(glycolic acid)]. *Polym. Int.* 54:36–46, 2005.

[3]Alvarez-Lopez, M., M. D. Pereda, J. A. DelValle, M. Fernandez-Lorenzo, M. C. Garcia-Alonso, O. A. Ruano, and M. L. Escudero. Corrosion behaviour of AZ31 magnesium alloy with different grain sizes in simulated biological fluids. *Acta Biomater.* 6:1763–1771, 2010.

[4]Arosio, P., V. Busini, G. Perale, D. Moscatelli, and M. Masi. A new model of resorbable device degradation and drug release—part I: zero order model. *Polym. Int.* 57:912–920, 2008.

[5]Biotronik, A. G. Safety and clinical performance of the drug eluting absorbable metal scaffold (DREAMS 2nd Generation) in the treatment of subjects with de Novo lesions in native coronary arteries: BIOSOLVE-II. In: ClinicalTrials.gov. Bethesda, MD: National Library of Medicine (US), 2000. Accessed 2015 May 15. Ⅽhttps://clinicaltrials.gov/ct2/show/NCT01960504.

[6]Bobel, A. C., S. Petisco, J. Ramon Sarasua, W. Wenxin, and P. E. McHugh. Computational bench testing to evaluate the short-term mechanical performance of a polymeric stent. *Cardiovasc. Eng. Technol.*, in press, 2015.

[7]Chen, Y., Z. Xu, C. Smith, and J. Sankar. Recent advances on the development of magnesium alloys for biodegradable implants. *Acta Biomater.* 10:4561–4573, 2014.

[8]Chen, Y., S. Zhou, and Q. Li. Mathematical modeling of degradation for bulk-erosive polymers: applications in tissue engineering scaffolds and drug delivery systems. *Acta Biomater.* 7:1140–1149, 2011.

[9]Cheng, Y., S. Deng, P. Chen, and R. Ruan. Polylactic acid (PLA) synthesis and modifications: a review. *Front. Chem. China* 4:259–264, 2009.

[10]Da Costa-Mattos, H. S., I. N. Bastos, and J. A. C. P. Gomes. A simple model for slow strain rate and constant load corrosion tests of austenitic stainless steel in acid aqueous solution containing sodium chloride. *Corros. Sci.* 50:2858–2866, 2008.

[11]Durand, E., T. Sharkawi, G. Leclerc, M. Raveleau, M. van der Leest, M. Vert, and A. Lafont. Head-to-head comparison of a drug-free early programmed dismantling polylactic acid bioresorbable scaffold and a metallic stent in the porcine coronary artery: six-month angiography and optical coherence tomographic follow-up study. *Circ. Cardiovasc. Interv.* 7:70–79, 2014.

[12]Farrar, D., and F. J. Buchanan. Chapter 9: modelling of the degradation processes for bioresorbable polymers. In: Degradation Rate of Bioresorbable Materials: Prediction and Evaluation, edited by D. Farrar. Amsterdam: Elsevier, 2008, pp. 183–206.

[13]Ferdous, J., V. B. Kolachalama, and T. Shazly. Impact of polymer structure and composition on fully resorbable endovascular scaffold performance. *Acta Biomater.* 9:6052–6061, 2013.

[14]Foin, N., R. D. Lee, R. Torii, J. L. Guitierrez-Chico, A. Mattesini, S. Nijjer, S. Sen, R. Petraco, J. E. Davies, C. Di Mario, M. Joner, R. Virmani, and P. Wong. Impact of stent strut design in metallic stents and biodegradable scaffolds. *Int. J. Cardiol.* 177:800–808, 2014.

[15]Food and Drug Administration. ASTM-FDA Workshop on Absorbable Medical Devices:Lessons Learned from Correlations of Bench Testing and Clinical Performance. 2012. Ⅽhttp://www.fda.gov/MedicalDevices/NewsEvents/WorkshopsConferences/ucm312601.htm.

[16]Friedrich, H. E., and B. L. Mordike. Magnesium Technology. Berlin: Springer, 2006.

[17]Fung, Y. C. Biomechanics: Mechanical Properties of Living Tissues. New York: Springer, 1981.

[18]Gastaldi, D., V. Sassi, L. Petrini, M. Vedani, S. Trasatti, and F. Migliavacca. Continuum damage model for bioresorbable magnesium alloy devices: application to coronary stents. *J. Mech. Behav. Biomed. Mater.* 4:352–365, 2011.

[19]Gogas, B. D., V. Farooq, Y. Onuma, and P. W. Serruys. The ABSORB bioresorbable vascular scaffold: an evolution or revolution in interventional cardiology. *Hell. J Cardiol* 53:301–309, 2012.

[20]Gopferich, A. Mechanisms of polymer degradation and erosion. *Biomaterials* 17:103–114, 1996.

[21]Grogan, J. A., D. Gastaldi, M. Castelletti, F. Migliavacca, G. Dubini, and P. E. McHugh. A novel flow chamber for biodegradable alloy assessment in physiologically realistic environments. *Rev. Sci. Instrum.* 84:094301, 2013.

[22]Grogan, J. A., S. B. Leen, and P. E. McHugh. Optimizing the design of a bioabsorbable metal stent using computer simulation methods. *Biomaterials* 34:8049–8060, 2013.

[23]Grogan, J. A., S. B. Leen, and P. E. McHugh. A physical corrosion model for bioabsorbable metal stents. *Acta Biomater.* 10:2313–2322, 2014.

[24]Grogan, J. A., S. B. Leen, and P. E. McHugh. Computational micromechanics of bioabsorbable magnesium stents. *J. Mech. Behav. Biomed. Mater.* 34:93–105, 2014.

[25]Grogan, J. A., B. J. O'Brien, S. B. Leen, and P. E. McHugh. A corrosion model for bioabsorbable metallic stents. *Acta Biomater.* 7:3523–3533, 2011.

[26]Han, X., and J. Pan. A model for simultaneous crystallisation and biodegradation of biodegradable polymers. *Biomaterials* 30:423–430, 2009.

[27]Haude, M., R. Erbel, P. Erne, S. Verheye, H. Degen, D. Böse, P. Vermeersch, I. Wijnbergen, N. Weissman, F. Prati, R. Waksman, and J. Koolen. Safety and performance of the drug-eluting absorbable metal scaffold (DREAMS) in patients with de-novo coronary lesions: 12 month results of the prospective, multicentre, first-in-man BIOSOLVE-I trial. *Lancet* 381:836–844, 2013.

[28]Hayman, D., C. Bergerson, S. Miller, M. Moreno, and J. E. Moore. The effect of static and dynamic loading on degradation of PLLA stent fibers. *J Biomech Eng* 136:4027614, 2014.

[29]Hermawan, H., D. Dubé, and D. Mantovani. Developments in metallic biodegradable stents. *Acta Biomater.* 6:1693–1697, 2010.

[30]Khan, K. A., and T. El-Sayed. A phenomenological constitutive model for the nonlinear viscoelastic responses of biodegradable polymers. *Acta Mech.* 224:287–305, 2013.

[31]Lin, Z., J. Luo, Z. Chen, J. Yi, H. Jiang, K. Tu, and L. Wang. A Monte Carlo simulation study of the effect of chain length on the hydrolysis of poly(lactic acid). *Chin. J. Polym. Sci.* 31:1554–1562, 2013.

[32]Luo, Q., X. Liu, Z. Li, C. Huang, W. Zhang, J. Meng, Z. Chang, and Z. Hua. Degradation model of bioabsorbable cardiovascular stents. *PLoS One* 9:e110278, 2014.

[33]Lyu, S., J. Schley, B. Loy, D. Lind, C. Hobot, R. Sparer, and D. Untereker. Kinetics and time–temperature equivalence of polymer degradation. *Biomacromolecules* 8:2301–2310, 2007.

[34]Lyu, S., and D. Untereker. Degradability of polymers for implantable biomedical devices. *Int. J. Mol. Sci.* 10:4033–4065, 2009.

[35]Mitra, A. K., and D. K. Agrawal. In stent restenosis: bane of the stent era. *J. Clin. Pathol.* 59:232–239, 2006.

[36]Moore, Jr, J., J. Soares, and K. Rajagopal. Biodegradable stents: biomechanical modeling challenges and opportunities. *Cardiovasc. Eng. Technol.* 1:52–65, 2010.

[37]Muliana, A., and K. R. Rajagopal. Modeling the response of nonlinear viscoelastic biodegradable polymeric stents. *Int. J. Solids Struct.* 49:989–1000, 2012.

[38]Murphy, J. G., R. S. Schwartz, K. C. Huber, and D. R. Holmes, Jr. Polymeric stents: modern alchemy or the future? *J. Invasive Cardiol.* 3:144–148, 1991.

[39]Okamura, T., P. W. Serruys, and E. Regar. Cardiovascular flashlight. The fate of bioresorbable struts located at a side branch ostium: serial three-dimensional optical coherence tomography assessment. *Eur. Heart J.* 31:2179, 2010.

[40]Ong, A. T. L., E. P. McFadden, E. Regar, P. P. T. De Jaegere, R. T. Van Domburg, and P. W. Serruys. Late angiographic stent thrombosis (LAST) events with drug-eluting stents. *J. Am. Coll. Cardiol.* 45:2088–2092, 2005.

[41]Ormiston, J. A., and P. W. S. Serruys. Bioabsorbable coronary stents. *Circ. Cardiovasc. Interv.* 2:255–260, 2009.

[42]Ormiston, J. A., M. W. Webster, and G. Armstrong. First-in-human implantation of a fully bioabsorbable drug-eluting stent: the BVS poly-L-lactic acid everolimus-eluting coronary stent. *Catheter Cardiovasc. Interv.* 69:128–131, 2007.

[43]Perale, G., P. Arosio, D. Moscatelli, V. Barri, M. Muller, S. Maccagnan, and M. Masi. A new model of resorbable device degradation and drug release: transient 1-dimension diffusional model. *J. Control Release* 136:196–205, 2009.

[44]Peuster, M., C. Hesse, T. Schloo, C. Fink, P. Beerbaum, and C. von Schnakenburg. Long-term biocompatibility of a corrodible peripheral iron stent in the porcine descending aorta. *Biomaterials* 27:4955–4962, 2006.

[45]Peuster, M., P. Wohlsein, M. Brügmann, M. Ehlerding, K. Seidler, C. Fink, H. Brauer, A. Fischer, and G. Hausdorf. A novel approach to temporary stenting: degradable cardiovascular stents produced from corrodible metal—results 6–18 months after implantation into New Zealand white rabbits. *Heart* 86:563–569, 2001.

[46]Pidaparti, R. M., L. Fang, and M. J. Palakal. Computational simulation of multi-pit corrosion process in materials. *Comput. Mater. Sci.* 41:255–265, 2008.

[47]Pitt, C. G., F. I. Chasalow, Y. M. Hibionada, D. M. Klimas, and A. Schindler. Aliphatic polyesters. I. The degradation of poly(ϵ-caprolactone) in vivo. *J. Appl. Polym. Sci.* 26:3779–3787, 1981.

[48]Prabhu, S., and S. Hossainy. Modeling of degradation and drug release from a biodegradable stent coating. *J. Biomed. Mater. Res. A* 80:732–741, 2007.

[49]Raabe, D., and R. C. Becker. Coupling of a crystal plasticity finite-element model with a probabilistic cellular automaton for simulating primary static recrystallization in aluminium. *Model. Simul. Mater. Sci. Eng.* 8:445–462, 2000.

[50]Rajagopal, K. R., A. R. Srinivasa, and A. S. Wineman. On the shear and bending of a degrading polymer beam. *Int. J. Plast.* 23:1618–1636, 2007.

[51]Rajagopal, K. R., and A. S. Wineman. A constitutive equation for nonlinear solids which undergo deformation induced microstructural changes. *Int. J. Plast.* 8:385–395, 1992.

[52]Schaffer, J. E., E. A. Nauman, and L. A. Stanciu. Cold drawn bioabsorbable ferrous and ferrous composite wires: an evaluation of in vitro vascular cytocompatibility. *Acta Biomater.* 9:8574–8584, 2013.

[53]Shazly, T., V. B. Kolachalama, J. Ferdous, J. P. Oberhauser, S. Hossainy, and E. R. Edelman. Assessment of material by-product fate from bioresorbable vascular scaffolds. *Ann. Biomed. Eng.* 40:955–965, 2012.

[54]Shirazi, R. N., F. Aldabbagh, A. Erxleben, Y. Rochev, and P. McHugh. Nanomechanical properties of poly(lactic-co-

glycolic) acid film during degradation. *Acta Biomater.* 10:4695–4703, 2014.

[55]Soares, J. S. Constitutive Modeling for Biodegradable Polymers for Application in Endovascular Stents. Doctoral dissertation, Texas A&M University, 2008.

[56]Soares, J. S., J. E. Moore, Jr, and K. R. Rajagopal. Constitutive framework for biodegradable polymers with applications to biodegradable stents. *ASAIO J.* 54:295–301, 2008.

[57]Soares, J. S., J. E. Moore, and K. R. Rajagopal. Modeling of deformation-accelerated breakdown of polylactic acid biodegradable stents. *J. Med. Device.* 4:41007, 2010.

[58]Soares, J., K. Rajagopal, and J. Moore Jr. Theoretical modeling of cyclically loaded, biodegradable cylinders. In: 3rd European Conference on Computational Mechanics, edited by C. A. Motasoares, J. A. C. Martins, H. C. Rodrigues, J. C. Ambrósio, C. A. B. Pina, C. M. Motasoares, E. B. R. Pereira, and J. Folgado. Netherlands: Springer, 2006, p. 207. doi:10.1007/1-4020-5370-3_207.

[59]Soares, J. S., K. R. Rajagopal, and J. E. Moore, Jr. Deformation-induced hydrolysis of a degradable polymeric cylindrical annulus. *Biomech. Model. Mechanobiol.* 9:177–186, 2010.

[60]Song, G., and A. Atrens. Corrosion mechanisms of magnesium alloys. *Adv. Eng. Mater.* 1:11–33, 1999.

[61]Sweeney, C. A., P. E. McHugh, J. P. McGarry, and S. B. Leen. Micromechanical methodology for fatigue in cardiovascular stents. *Int. J. Fatigue* 44:202–216, 2012.

[62]Tamai, H., K. Igaki, E. Kyo, K. Kosuga, A. Kawashima, S. Matsui, H. Komori, T. Tsuji, S. Motohara, and H. Uehata. Initial and 6-month results of biodegradable poly-L-lactic acid coronary stents in humans. *Circulation* 102:399–404, 2000.

[63]Tormala, P., T. Pohjonen, and P. Rokkanen. Bioabsorbable polymers: materials technology and surgical applications. *Proc. Inst. Mech. Eng. H* 212:101–111, 1998.

[64]Verheye, S., M. Webster, J. Stewart, A. Abizaid, R. Costa, J. Costa, J. Yan, V. Bhat, L. Morrison, S. Toyloy, and J. Ormiston. TCT-563 multi-center, first-in-man evaluation of the myolimus-eluting bioresorbable coronary scaffold: 6-month clinical and imaging results. *J. Am. Coll. Cardiol.* 60:B163, 2012.

[65]Waksman, R. Absorbable Metal Stent, Clinical Update and DREAMS: Concept and Preclinical Data. Tel-Aviv: Innovations of Cardiovascular Interventions, 2007.

[66]Waksman, R., R. Erbel, C. Di Mario, J. Bartunek, B. de Bruyne, F. R. Eberli, P. Erne, M. Haude, M. Horrigan, C. Ilsley, D. Böse, H. Bonnier, J. Koolen, T. F. Lüscher, and N. J. Weissman. Early- and long-term intravascular ultrasound and angiographic findings after bioabsorbable magnesium stent implantation in human coronary arteries. *JACC Cardiovasc. Interv.* 2:312–320, 2009.

[67]Waksman, R., R. Pakala, R. Baffour, R. Seabron, D. Hellinga, and F. O. Tio. Short-term effects of biocorrodible iron stents in porcine coronary arteries. *J. Interv. Cardiol.* 21:15–20, 2008.

[68]Wang, Y., J. Pan, X. Han, C. Sinka, and L. Ding. A phenomenological model for the degradation of biodegradable polymers. *Biomaterials* 29:3393–3401, 2008.

[69]Weir, N. A., F. J. Buchanan, J. F. Orr, and G. R. Dickson. Degradation of poly-L-lactide. Part 1: in vitro and in vivo physiological temperature degradation. *Proc. Inst. Mech. Eng. H* 218:307–319, 2004.

[70]Witte, F., J. Fischer, J. Nellesen, H. A. Crostack, V. Kaese, A. Pisch, F. Beckmann, and H. Windhagen. In vitro and in vivo corrosion measurements of magnesium alloys. *Biomaterials* 27:1013–1018, 2006.

[71]Wu, W., S. Chen, D. Gastaldi, L. Petrini, D. Mantovani, K. Yang, L. Tan, and F. Migliavacca. Experimental data confirm numerical modeling of the degradation process of magnesium alloys stents. *Acta Biomater.* 9:8730–8739, 2013.

[72]Wu, W., D. Gastaldi, K. Yang, L. Tan, L. Petrini, and F. Migliavacca. Finite element analyses for design evaluation of biodegradable magnesium alloy stents in arterial vessels. *Mater. Sci. Eng. B Solid-State Mater. Adv. Technol.* 176:1733–1740, 2011.

[73]Wu, W., L. Petrini, D. Gastaldi, T. Villa, M. Vedani, E. Lesma, B. Previtali, and F. Migliavacca. Finite element shape optimization for biodegradable magnesium alloy stents. *Ann. Biomed. Eng.* 38:2829–2840, 2010.

[74]Zartner, P., R. Cesnjevar, H. Singer, and M. Weyand. First successful implantation of a biodegradable metal stent into the left pulmonary artery of a preterm baby. *Catheter. Cardiovasc. Interv.* 66:590–594, 2005.

[75]Zheng, Y. F., X. N. Gu, and F. Witte. Biodegradable metals. *Mater. Sci. Eng. R Reports* 77:1–34, 2014.